SINR Model for MBSFN Based Mission Critical Communications

Alaa Daher[1,2], Marceau Coupechoux[2], Philippe Godlewski[2], Jean-Marc Kelif [3], Pierre Ngouat[4] and Pierre Minot[1]
[1]ETELM, Les Ulis, France; {alaa.daher,pierre.minot}@etelm.fr
[2]LTCI, Telecom ParisTech, University Paris-Saclay, France
{alaa.daher, marceau.coupechoux, philippe.godlewski}@telecom-paristech.fr
[3]Orange Labs, Issy-Les-Moulineaux, France; jeanmarc.kelif@orange.com
[4]PNG-Technologies, Torcy, France; pierre.ngouat@png-technologies.com

***Abstract*—Multicast/Broadcast Single Frequency Network (MBSFN) is envisioned to be a key technology for business and mission critical communications. The need arises to define simple and efficient dimensioning rules for such networks. The Signal to Interference plus Noise Ratio (SINR) is an important key performance parameter since other metrics such as outage probability and capacity can be deduced from it. In this work, we propose an analytical model to derive an approximate closed-form formula of the SINR in a MBSFN. Our model takes into account Inter-Symbol Interference due to the different propagation delays between the User Equipment (UE) and its serving evolved Nodes-B (eNBs). The comparison with Monte Carlo simulations shows that our approach provides accurate results when shadowing standard deviation is low. When shadowing is highly variable, our model, while less accurate, outperforms the traditional approach based on Fenton-Wilkinson. This phenomenon is due to the fact that several eNBs serve the same UE so that shadowing on every individual link compensate.**

I. Introduction

Business and mission critical communications are communications between professional users, either from the public safety sector, or operating critical infrastructures. Currently, these communications rely on Professional Mobile Radio (PMR) networks owing to special requirements and services for professional users. PMR networks are mainly devoted to provide voice services, whereas the provision of new multimedia services, which require higher data rates (e.g. video streaming), is now required. In this context, the adoption of the commercial broadband networks, such as Long Term Evolution Advanced (LTE-A), to convey PMR services is a viable solution. Thus, 3rd Generation Partnership Project (3GPP) Release 12 has started including public safety features [1].

Group communication is the main service allowed by PMR networks. 3GPP has introduced the evolved Multimedia Multicast/Broadcast Service (eMBMS) as a point-to-multipoint content delivery solution for LTE, to enhance flexibility and spectrum efficiency when providing broadcast and multicast services. This can be achieved through increased performance of the air interface, by introducing the Multicast/Broadcast Single Frequency Network (MBSFN) transmission, based on simultaneous transmission of eMBMS data, from multiple synchronized evolved Nodes-B (eNBs).

Radio network planning is one of the key steps before deployment. Dimensioning tools are based on the characterization of the Signal to Interference plus Noise Ratio (SINR), which allows the derivation of outage probabilities, as well as the evaluation of system capacity. The need thus arises for simple, fast and accurate method to compute the SINR as a function of the main network parameters.

The SINR has been evaluated analytically in the literature for single-cell as well as multi-cell transmissions. In [2], authors propose a model for Inter-Symbol Interference (ISI) in a MBSFN network but do not provide a model for the SINR. Ohmann et al. provide in [3] an approximate SINR distribution but don't take into account ISI and do not provide a simple closed-form formula for the SINR as a function of the distance between the User Equipment (UE) and its closest serving eNB.

Our work is inspired by [4], [5]. In [4], a fluid model is proposed to evaluate the so called other-cell interference factor, and a closed-form formula has been provided to derive outage probability. Furthermore, authors of [5] derive an analytical formula of the Signal to Interference Ratio (SIR) using Fenton-Wilkinson approach, considering the shadowing impact. However, both studies consider single-cell transmissions, while our evaluation studies MBSFN, a multi-cell transmission technique.

In this paper, we introduce an analytical model, that allows quick calculations of the SINR in MBSFN transmissions. We show that our model matches well Monte Carlo simulations when shadowing standard deviation is low. When shadowing standard deviation increases, our model becomes less accurate but outperforms the Fenton-Wilkinson approach [6] used in literature to evaluate the shadowing impact. We show that our model is simpler and provides more accurate results.

The paper is organized as follows: in section II, we introduce MBSFN and the network model. We define our analytical model and apply Fenton-Wilkinson in section III. Section IV presents and discusses the simulation results. Finally, conclusions are summarized in section V.

II. System model

Evolved MBMS data can be delivered either by unicast or Point-To-Multipoint (PTM) transmissions. In the latter, a common channel is used to simultaneously convey the information to multiple (multicast transmission) or all (broadcast transmission) UEs requesting the data. Hence, 3GPP has introduced the MBSFN as a technique for PTM transmissions in LTE Release 9. In the following sections, we present the network model for MBSFN transmissions and SINR calculations.

A. Network model

MBSFN has been defined as a downlink multi-cell transmission technique, where a time-synchronized common waveform is transmitted from multiple cells, which leads to significant improvement in SINR. The group of eNBs which contribute to the simulcast transmission constitutes the so-called MBSFN area [7]. Moreover, MBSFN networks can support a group of reserved cells; such a cell may be allowed to transmit for other services on the resource allocated to MBSFN transmission, but at restricted power. Let $\mathcal{X}$ the set of all cells (or eNBs) in the network, $\mathcal{X}_t$ the set of eNBs inside the MBSFN area, $\mathcal{X}_r$ the set of reserved cells, and $\mathcal{X}_o$ the set of other cells not involved in MBSFN transmission. Hence, $\mathcal{X} = \mathcal{X}_t \cup \mathcal{X}_r \cup \mathcal{X}_o$, see Figure 1.

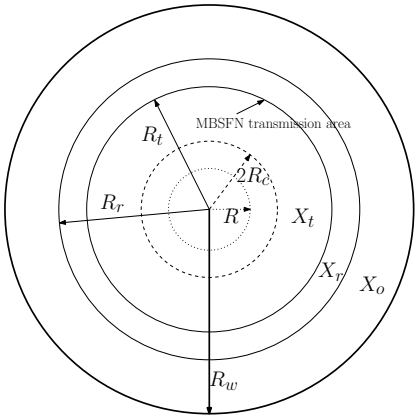

Fig. 1: MBSFN network model.

B. SINR evaluation

In MBSFN, the signal received from an eNB of the MBSFN area is part of the useful received signal, provided that the propagation delay does not exceed the Cyclic Prefix (CP) duration. To account for this, we define the weight function of the useful portion of a received MBSFN signal as [2]:

$$\omega(\tau_{bm}) = \begin{cases} 0 & \tau_{bm} < -T_u \\ 1 + \dfrac{\tau_{bm}}{T_u} & -T_u \leq \tau_{bm} < 0 \\ 1 & 0 \leq \tau_{bm} < T_P \\ 1 - \dfrac{\tau_{bm} - T_{CP}}{T_u} & T_P \leq \tau_{bm} < T_P + T_u \\ 0 & \text{otherwise} \end{cases} \quad (1)$$

where τ_{bm} is the difference in propagation delay between signals from the eNB b and the serving eNB 0 at UE m, i.e., $\tau_{bm} = \frac{r_{bm} - r_{0m}}{c}$, where r_{im} denotes the distance between UE m and eNB i, and c is the light propagation speed. Parameter T_u is the duration of the useful part of Orthogonal Frequency-Division Multiplexing (OFDM) symbol and T_P is the CP duration.

Assume that the distance r_0 to the closest serving eNB is known and serves as a reference for other signals, then this weight function can be modified for any eNB at a distance r from the UE as follows:

$$\Gamma(r, r_0) = \begin{cases} 1 & r_0 \leq r < r_0 + cT_P \\ -\dfrac{r - r_0 - c(T_P + T_u)}{cT_u} & r_0 \leq r - cT_P < r_0 + cT_u \\ 0 & \text{otherwise} \end{cases} \quad (2)$$

Therefore, the SINR experienced by UE m can be expressed by:

$$\gamma_m = \frac{p_{t,u}(m)}{p_{t,i}(m) + p_{o,i}(m) + N} \quad (3)$$

where $p_{t,u}(m)$ and $p_{t,i}(m)$ denotes respectively the sum of useful and interference portions of signals received from eNBs in $\mathcal{X}_t$, while $p_{o,i}(m)$ refers to the power of received signals transmitted by eNBs in $\mathcal{X}_o$. Parameter N is the thermal noise power given by $N = N_0 W$, where N_0 denotes the white noise power spectral density, and W the system bandwidth. Now useful and interfering signal powers can be written as:

$$p_{t,u}(m) = \sum_{b \in \mathcal{X}_t} \omega(\tau_{bm}) P_b K r_{bm}^{-\eta} X_{bm} \quad (4)$$

$$p_{t,i}(m) = \sum_{b \in \mathcal{X}_t} (1 - \omega(\tau_{bm})) P_b K r_{bm}^{-\eta} X_{bm} \quad (5)$$

$$p_{o,i}(m) = \sum_{b \in \mathcal{X}_o} P_b K r_{bm}^{-\eta} X_{bm}, \quad (6)$$

where P_b is the transmit power of eNB b assumed to be constant across eNBs; K is a constant; η is the path-loss exponent (η is typically strictly greater than 2 and for technical reasons we assume $\eta \neq 3$); $X_{bm} = 10^{\xi_{bm}/10}$ is a log-normal Random Variable (RV) characterizing shadowing; ξ_{bm} is a zero-mean gaussian RV with standard deviation σ in dB.

III. Analytical approach

In this section, we extend the fluid model presented in [4], [5] to MBSFN.

A. Analytical model

The fluid model approach, developed in [4], consists in replacing a given fixed discrete number of transmitters (eNBs) by an equivalent continuum of transmitters over the network area. In MBSFN, this approach means that the useful and interference portions of signals transmitted by eNBs inside the MBSFN area ($\mathcal{X}_t$), in addition to interference signals received from interfering eNBs outside of MBSFN area ($\mathcal{X}_o$) are now

considered as continuum fields. In a homogeneous and regular cellular network, we denote ρ the constant eNB density.

We first consider a central cell of radius R (see Figure 1). Around this cell, there is a MBSFN area of radius $R_t \geq R_c$ (R_c is the half inter-eNB distance). Around this area, there is a ring of reserved cells between disks of radius R_t and R_r. At last, the network is assumed to be a disk of radius $R_n \geq R_r$.

In a first approach, we ignore shadowing and approximate in (3) every sum by an integral:

$$\begin{aligned} p_{o,i}(r_0) &= \int_0^{2\pi} \int_{R_r - r_0}^{R_n - r_0} \rho P_b K r^{-\eta} r dr d\theta \\ &= 2\pi\rho P_b K \frac{(R_r - r_0)^{2-\eta} - (R_n - r_0)^{2-\eta}}{\eta - 2}, \end{aligned} \quad (7)$$

where r_0 is the distance between UE m and its serving eNB of index 0 from which m receives the highest power, and r is the distance from m to a given transmitting position. Received powers can now be expressed as functions of the single variable r_0. We apply the same technique to $p_{t,u}(m)$ and $p_{t,i}(m)$:

$$\begin{aligned} p_{t,u}(r_0) &= P_b K r_0^{-\eta} + \int_0^{2\pi} \int_{2R_c - r_0}^{R_t - r_0} \rho P_b K \Gamma(r, r_0) r^{-\eta} r dr d\theta \\ &= 2\pi\rho P_b K \left(\frac{r_0^{-\eta}}{2\pi\rho} + \frac{(2R_c - r_0)^{2-\eta}}{\eta - 2} - \Phi(r_0) \right) \end{aligned} \quad (8)$$

$$\begin{aligned} p_{t,i}(r_0) &= \int_0^{2\pi} \int_{2R_c - r_0}^{R_t - r_0} \rho P_b K (1 - \Gamma(r, r_0)) r^{-\eta} r dr d\theta \\ &= 2\pi\rho P_b K \left(\Phi(r_0) - \frac{(R_t - r_0)^{2-\eta}}{\eta - 2} \right) \end{aligned} \quad (9)$$

where $\Phi(r_0)$ is defined as follows:

$$\Phi(r_0) = \frac{(2R_c - r_0)^{2-\eta}}{\eta - 2} - \int_{2R_c - r_0}^{R_t - r_0} \Gamma(r, r_0) r^{-\eta} r dr \quad (10)$$

To evaluate these integrals, we consider several sub-cases.

1) $r_0 > \frac{R_t - cT_P}{2}$*:* The signals transmitted by eNBs $b \in \mathcal{X}_t$ arrive at UE m with no excessive delay; thus, these signals are totally useful. In this case:

$$\Phi(r_0) = \frac{(R_t - r_0)^{2-\eta}}{\eta - 2} \quad (11)$$

2) $\frac{2R_c - cT_P}{2} < r_0 < \frac{R_t - c(T_P + T_u)}{2}$*:* In this case, the first ring around eNB 0 contributes only to the useful signal, while other eNBs from the MBSFN area may contribute to the interference depending on their distance to the UE. We obtain:

$$\Phi(r_0) = \frac{[r_0 + cT_P]^{3-\eta} - [r_0 + c(T_P + T_u)]^{3-\eta}}{cT_u(\eta - 2)(\eta - 3)} \quad (12)$$

3) $\frac{2R_c - cT_P}{2} < r_0$ *and* $\frac{R_t - c(T_P + T_u)}{2} < r_0 < \frac{R_t - cT_P}{2}$*:* In this case, all eNBs from the MBSFN area are interfering except the first ring, which contributes only to useful signal. We obtain (13).

4) $r_0 < \frac{R_t - c(T_P + T_u)}{2}$ *and* $\frac{2R_c - c(T_P + T_u)}{2} < r_0 < \frac{2R_c - cT_P}{2}$*:* All eNBs $b \in \mathcal{X}_t$ signals, including the first ring, have useful and interfering parts. We obtain (14).

5) $r_0 > \frac{R_t - c(T_P + T_u)}{2}$ *and* $\frac{2R_c - c(T_P + T_u)}{2} < r_0 < \frac{2R_c - cT_P}{2}$*:* Only the signals received from first ring eNBs include useful and interfering portions, while the signals transmitted from other eNBs in the MBSFN area are completely interfering. We obtain (15).

6) $r_0 \leq \frac{2R_c - c(T_P + T_u)}{2}$*:* In this case, all signals transmitted by eNBs $b \in \mathcal{X}_t \backslash \{0\}$ arrive with excessive delays, so that they completely interfere with the signal transmitted by the serving eNB. Thus:

$$\Phi(r_0) = \frac{(2R_c - r_0)^{2-\eta}}{\eta - 2} \quad (16)$$

B. Fenton-Wilkinson Approach for Shadowing

In this section, we propose an approximation of the SINR in MBSFN transmissions based on Fenton-Wilkinson method, in order to analyze the shadowing impact. Indeed, in [5], the method called FWBM, which approximates a sum of lognormal by a lognormal, exhibits accurate results in single-cell transmissions.

Assuming that all eNBs transmit with the same power P_b, the SINR in (3) can be formulated as in (17), where f_u, f_i and f_N denote useful, interference and noise factors respectively. To compute the characteristics of these factors, let us define the following functions:

$$\begin{aligned} f(\boldsymbol{\omega}, \boldsymbol{r}, \eta, \mathcal{X}) &= \sum_{i \in \mathcal{X}} \omega_i r_i^{-\eta} \\ H(\boldsymbol{\omega}, \boldsymbol{r}, \eta, \sigma, \mathcal{X}) &= \left((e^{a^2\sigma^2/2} - 1) \frac{\sum_{i \in \mathcal{X}} \omega_i^2 r_i^2}{(\sum_{i \in \mathcal{X}} \omega_i r_i)^2} + 1 \right)^{-\frac{1}{2}} \end{aligned} \quad (18)$$

where $a = ln(10)/10$, $\mathcal{X}$ denotes a set of eNBs, $\boldsymbol{\omega}$ and $\boldsymbol{r}$ are two vectors representing the weighting function and the distance between UE m and every element of $\mathcal{X}$. Using Fenton-Wilkinson approach [6], we approximate f_u, f_i and f_N as lognormal RVs. Thus, equations (19), (20) and (21) provides the corresponding mean and variance respectively:

$$\begin{aligned} a\mu_u &= ln \left(\frac{f(1 - \omega(\tau), r, \eta, \mathcal{X}_t)}{f(\omega(\tau), r, \eta, \mathcal{X}_t)} \cdot \frac{H(1 - \omega(\tau), r, \eta, \sigma, \mathcal{X}_t)}{H(\omega(\tau), r, \eta, \sigma, \mathcal{X}_t)} \right) \\ a^2\sigma_u^2 &= -2ln \left[H(1 - \omega(\tau), r, \eta, \sigma, \mathcal{X}_t) . H(\omega(\tau), r, \eta, \sigma, \mathcal{X}_t) \right] \end{aligned} \quad (19)$$

$$\begin{aligned} a\mu_i &= ln \left(\frac{f(\mathbf{1}, r, \eta, \mathcal{X}_o)}{f(\omega(\tau), r, \eta, \mathcal{X}_t)} \frac{H(\mathbf{1}, r, \eta, \sigma, \mathcal{X}_o)}{H(\omega(\tau), r, \eta, \sigma, \mathcal{X}_t)} \right) \\ a^2\sigma_i^2 &= -2ln \left[H(\mathbf{1}, r, \eta, \sigma, \mathcal{X}_o) . H(\omega(\tau), r, \eta, \sigma, \mathcal{X}_t) \right] \end{aligned} \quad (20)$$

Finally, we determine the mean and variance of γ_m as follows:

$$\begin{aligned} a\mu_{\gamma_m} &= -\left[ln \left(\sum_{l \in \{u,i,N\}} e^{a\mu_l + a^2\sigma_l^2/2} \right) - \frac{a^2\sigma_{\gamma_m}^2}{2} \right] \\ a^2\sigma_{\gamma_m}^2 &= ln \left[\frac{\sum_{l \in \{u,i,N\}} (e^{a^2\sigma_l^2} - 1) e^{2a\mu_l + a^2\sigma_l^2}}{(\sum_{l \in \{u,i,N\}} e^{a\mu_l + a^2\sigma_l^2/2})^2} + 1 \right] \end{aligned} \quad (22)$$

IV. Simulation

In this section, we compare our model to Monte Carlo simulations and compare it to the Fenton-Wilkinson approach.

$$\Phi(r_0) = \frac{(r_0 + cT_P)^{3-\eta}}{cT_u(\eta-2)(\eta-3)} + \frac{r_0 + c(T_P+T_u)}{cT_u}\frac{(R_t - r_0)^{2-\eta}}{\eta-2} - \frac{(R_t-r_0)^{3-\eta}}{cT_u(\eta-3)} \tag{13}$$

$$\Phi(r_0) = \frac{(2R_c - r_0)^{3-\eta}}{cT_u(\eta-3)} - \frac{r_0 + cT_P}{cT_u}\frac{(2R_c-r_0)^{2-\eta}}{\eta-2} - \frac{(r_0 + c(T_P+T_u))^{3-\eta}}{cT_u(\eta-2)(\eta-3)} \tag{14}$$

$$\Phi(r_0) = \frac{(2R_c - r_0)^{3-\eta} - (R_t-r_0)^{3-\eta}}{cT_u(3-\eta)} - \frac{r_0 + cT_P}{cT_u}\frac{(2R_c-r_0)^{2-\eta}}{\eta-2} + \frac{r_0 + c(T_P+T_u)}{cT_u}\frac{(R_t-r_0)^{2-\eta}}{\eta-2} \tag{15}$$

$$\gamma_m = \left(\frac{\sum_{b\in\mathcal{X}_t}(1-\omega(\tau_{bm}))r_{bm}^{-\eta}X_{bm}}{\sum_{b\in\mathcal{X}_t}\omega(\tau_{bm})r_{bm}^{-\eta}X_{bm}} + \frac{\sum_{b\in\mathcal{X}_o} r_{bm}^{-\eta}X_{bm}}{\sum_{b\in\mathcal{X}_t}\omega(\tau_{bm})r_{bm}^{-\eta}X_{bm}} + \frac{N}{\sum_{b\in\mathcal{X}_t}\omega(\tau_{bm})P_bKr_{bm}^{-\eta}X_{bm}} \right)^{-1} = (f_u + f_i + f_N)^{-1} \tag{17}$$

A. Simulation Parameters

We consider a hexagonal urban city cellular network composed of a central cell and 10 rings of adjacent eNBs (331 omni-directional eNBs in total). The UEs are distributed in the MBSFN area, formed by the central cell in addition to 2 rings of adjacent cells (reserved cells are not considered in this first setting). Hata model (Urban, eNB antenna height of 55 m, UE antenna height of 1.5 m) is assumed for path-loss evaluations. The system simulation parameters that were taken into account for our simulations are presented in Table I.

Parameter	Assumption
System model	Macro-cells, urban city
Cellular layout	331 eNBs, omnidirectional
Carrier frequency (f_c)	800 MHz
Duplex method and Bandwidth	FDD, 5 MHz
eNB Tx power	40dBm (10W)
Cell range (R)	1.5 Km, 3 Km or 5 Km
eNB density (ρ)	$(3\sqrt{3}R^2/2)^{-1}$
Half distance between 2 eNBs (R_c)	$R\sqrt{3}/2$
MBSFN area radius (R_t)	$5R\sqrt{3}/2$
White noise power spectral density (N_0)	-174 dBm/Hz
Shadowing standard deviation (σ)	3dB, 6dB or 8dB
Cyclic Prefix length, T_P	16.7 µs
Useful signal frame length, T_u	66.7 µs

TABLE I: Simulation parameters.

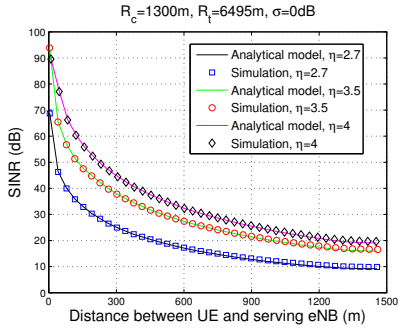

Fig. 2: Comparison of the analytical model with simulations assuming path-loss exponents $\eta = 2.7$, 3.5 and 4.

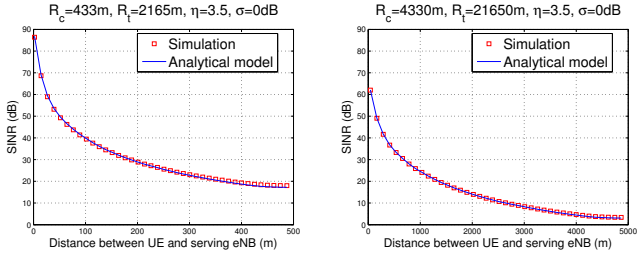

(a) $R = 500$ m (b) $R = 5000$ m

Fig. 3: Comparison of the analytical model with simulations assuming cell ranges $R = 500$ m and 5000 m.

B. Deterministic Path-Loss

Figure 2 shows the comparison between the analytical model and the SINR evaluated by simulations without shadowing ($\sigma = 0$ dB), for different path-loss exponent η. We observe that the analytical model matches very well the simulations, for different realistic values of η.

In Figure 3, we show that our model is accurate for various cell ranges, from 500 m (as envisioned for mission critical deployments) to 5000 m (a typical value for classical MBSFN networks).

Moreover, we evaluate our analytical model for different MBSFN configurations. We consider two different configurations: in the first one, only the first ring of adjacent eNBs transmit the MBSFN signals, while in the second, we assume two rings of transmitting cells with an additional single ring of reserved cells, which do not transmit on MBSFN resources. Figure 4 shows that in both configuration the model matches well the simulation results.

C. Impact of Shadowing

In this section, the SINR is evaluated by simulation by taking into consideration the impact of shadowing. We also

$$
\begin{aligned}
a\mu_N &= -\left[ln\frac{PK}{N} + lnf(\omega(\tau), r, \eta, \mathcal{X}_t) + \frac{a^2\sigma^2}{2} + lnH(\omega(\tau), r, \eta, \sigma, \mathcal{X}_t)\right] \\
a^2\sigma_N^2 &= -2lnH(\omega(\tau), r, \eta, \sigma, \mathcal{X}_t)
\end{aligned} \tag{21}
$$

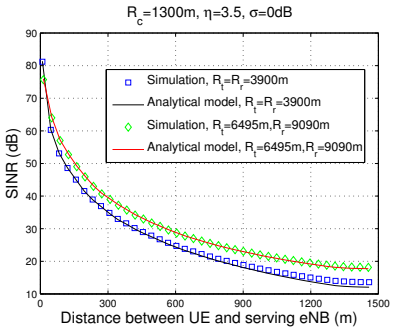

Fig. 4: Comparison of the analytical model with simulations assuming different MBSFN area configurations.

assume a best server policy, i.e., the reference serving eNB for a UE is the one providing the highest useful received signal. We compare these simulations with our model and with the Fenton-Wilkinson approach. In the latter method, μ_{γ_m} as in (22) is plotted as a function of the distance to the reference serving eNB. Figure 5 shows the variation of the SINR with respect to the distance to the serving eNB (left) and the Complementary Distribution Function (CDF) of the SINR (right) for various realistic shadowing standard deviations. As expected, the accuracy of the two approaches decreases with increasing σ. For $\sigma = 3$ dB, our model matches very well with simulations. There is at most 3 dB difference at $\sigma = 6$ dB. The maximum difference reaches 5 dB for $\sigma = 8$ dB (at 500 m from the eNB). In terms of CDF, our model is more accurate for high SINRs than for very low SINRs. However, in all cases our analytical model does better than Fenton-Wilkinson, which is the reference method in the literature for taking into account shadowing. Owing to its simplicity, our model can be preferred.

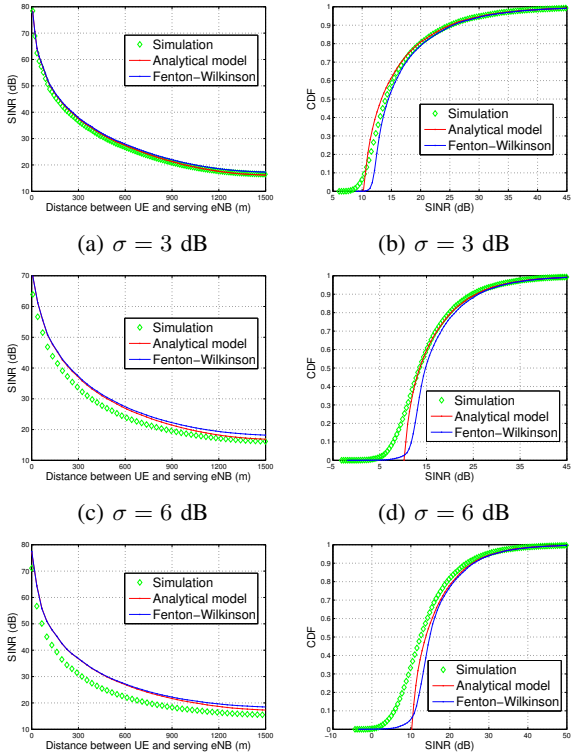

(a) $\sigma = 3$ dB (b) $\sigma = 3$ dB

(c) $\sigma = 6$ dB (d) $\sigma = 6$ dB

(e) $\sigma = 8$ dB (f) $\sigma = 8$ dB

Fig. 5: Comparison of the analytical model with Monte Carlo simulations and Fenton-Wilkinson approach assuming $R = 1500$ m, $\eta = 3.5$ and $\sigma = 3$, 6 and 8 dB. Left: SINR as a function of UE-eNB distance. Right: CDF of the SINR.

V. Conclusion

In this paper, we have proposed a SINR model for MBSFN based mission critical communications. Our model takes into account Inter-Symbol Interference as well as the MBSFN area size. Closed-form formulas for the expression of the SINR as a function of the distance to the nearest serving eNode-B makes the proposed model particularly appealing for fast dimensioning processes. Monte Carlo simulations show that our approach is very accurate when shadowing is low. At high shadowing standard deviation, our model does better than the classical Fenton-Wilkinson approach.

References

[1] Huawei, HiSilicon, TD-Tech, SouthernLINC, Potevio, China Unicom, MediaTek Inc., CATT, "Comparison of SC-PTM and MBSFN use for Public Safety," TSG R2-151516, 3GPP, Apr. 2015.

[2] L. Rong, O. B. Haddada, and S. E. Elayoubi, "Analytical analysis of the coverage of a MBSFN OFDMA network," *GLOBECOM - IEEE Global Telecommunications Conference*, pp. 2388–2392, 2008.

[3] D. Ohmann, A. Awada, I. Viering, M. Simsek, and G. P. Fettweis, "Best server SINR models for single-and multi-point transmission in wireless networks," in *2015 IEEE Global Communications Conference, GLOBECOM 2015*, 2016.

[4] J. M. Kelif, M. Coupechoux, and P. Godlewski, "Spatial outage probability for cellular networks," *GLOBECOM - IEEE Global Telecommunications Conference*, pp. 4445–4450, 2007.

[5] D. Ben Cheikh, J.-M. Kelif, M. Coupechoux, and P. Godlewski, "SIR distribution analysis in cellular networks considering the joint impact of path-loss, shadowing and fast fading," *EURASIP Journal on Wireless Communications and Networking*, vol. 2011, no. 1, p. 137, 2011.

[6] L. F. Fenton, "The Sum of Log-Normal Probability Distributions in Scatter Transmission Systems," *IRE Transactions on Communications Systems*, vol. 8, no. 1, pp. 57–67, 1960.

[7] 3GPP, "Evolved Universal Terrestrial Radio Access (E-UTRA) and Evolved Universal Terrestrial Radio Access Network (E-UTRAN): Overall description," TS 36.300, 3GPP, Dec. 2015.